

## A NEW ENERGY INDICATOR IN DAMAGE LOCATING VECTOR METHOD (DLV) FOR DETECTING MULTIPLE DAMAGED POSITIONS IN BEAM AND TRUSS STRUCTURES

Nguyen Minh Nhan<sup>1</sup>, Dinh Cong Du<sup>1</sup>, Vo Duy Trung<sup>1</sup>,  
Tran Viet Anh<sup>1</sup>, Nguyen Thoi Trung<sup>2,\*</sup>

<sup>1</sup>Ton Duc Thang University, Ho Chi Minh City, Vietnam

<sup>2</sup>University of Science, Vietnam National University - Ho Chi Minh City, Vietnam

\*E-mail: thoitruong76@gmail.com

Received January 08, 2015

**Abstract.** The paper presents a new indicator called normalized energy index (*nei*) in damage locating vector method (DLV) for detecting multiple damaged positions in beam and truss structures. In the DLV method, a set of load vectors, which is extracted from the change in flexibility matrix between an undamaged structure and a damaged one, is applied as static loads to the undamaged structure which are evaluated via the finite element modeling. Then, the *nei* values are computed for each element by using the displacements. In order to verify the accuracy and efficiency of a proposed indicator, a cantilevered beam and a 14-bay planar truss are considered.

**Keywords:** Damage locating vector method (DLV), strain energy, load vector, damage detection, vibration.

### 1. INTRODUCTION

Structural health monitoring (SHM) is being considered as a promising field when the safety of structures is considered in construction engineering. In SHM, it is important to detect the location of the damage as well as its extent. In numerical simulation, the damage in structures is usually simulated as the reduction of elemental stiffness. The weakening of structural members usually comes along with the changes in dynamic characteristics of structures which compose of frequencies and mode shapes. These characteristics are usually captured in a vibrating structure which is excited by either wind, or moving vehicle, earthquake or shaker. Based on the modal properties, scientists have developed many different methods to identify damaged elements and their severities.

Cawley and Adams [1] proposed natural frequency shift as an indicator for identifying and quantifying damage in structures. Salawu and Williams [2] used a robust tool namely modal assurance criterion (MAC) [3] for damage detection in a reinforced concrete bridge. The test showed that MAC was more sensitive than the natural frequency shift. Pandey and Biswas [4] proposed a method where the change of mode shape curvature defined as second order derivative of deflection had been used to locate damage in a finite element beam structure. The change is understood as the difference between an intact modal (reference modal) and a damaged modal. This method was further developed by focusing on the change in flexibility matrix (inverse of stiffness matrix) [5–7]. A damage index method based on the difference of modal strain energy between reference and damaged structural model was introduced by Stubbs and Kim [8]. In addition to the above modal based damage identification methods, there are some other methods that can be found in excellent reviews [9–11] such as the optimal matrix update methods [12, 13], wavelet transform methods [14–16], the neural network-based methods [17, 18], etc.

Recently, among damage localization methods using the change in flexibility matrix, the damage locating vector method (DLV) [19] was developed and applied to many types of structures namely: beam, truss and frame structures. In the DLV method, some load vectors designed as damage locating vectors (DLVs) are sought and applied to reference structures. The crucial feature of these loads is that they cause zero stress in damaged elements of structures. This feature helped identify damage in structures. Particularly, an indicator called normalized cumulative stress (*ncs*) was proposed to detect damage. From the formulation of the DLV method, there are three remarkable advantages: (1) the obtained DLVs would be applied into reference model which can be easily computed using finite element analysis (FEA); (2) the limited sensors issue in data measurement can be solved efficiently; and (3) the DLV method can be applied to both static and dynamic measurements. As a result, the DLV method became a favorite subject for researchers. For instance, in 2007, Gao et al. [20] progressed successfully an experiment on fifteen-feet truss. In 2009, Quek et al. [21] enhanced the DLV method by proposing a new indicator called normalized cumulative energy (*nce*) and an algorithm to adapt to the case of limited sensors.

In this study, the normalized strain energy (*nce*) in DLV method is modified and presented as normalized energy index (*nei*). The technique in modifying can be found in Seyedpoor [22] and Nobahari [23] where two indexes namely modal strain energy based index (MSEBI) and flexibility strain energy based index (FSEBI) are computed using strain energy of mode shapes and displacements in flexibility matrix, respectively. Theoretically, *nei* shows similar results with the original *ncs* as well as the recently proposed *nce*, thought, its formulation is simpler. In order to demonstrate the efficiency of *nei*, three numerical examples of cantilevered beam, 14-bay planar truss, and 72-bar space truss are considered.

## 2. FORMULATION OF NORMALIZED ENERGY INDEX IN DLV METHOD

Three well-known concepts in damage detection methods namely: (1) flexibility matrix, (2) damage locating vectors (DLVs), and (3) strain energy will be used to formulate the normalized energy index (*nei*) as follows:

From modal properties of structure, the flexibility matrix is computed as follows [6]

$$\mathbf{F} = \sum_{i=1}^{s dof} \frac{1}{\omega_i^2} \mathbf{\Phi}_i \mathbf{\Phi}_i^T, \quad (1)$$

where  $\mathbf{F}$  is the flexibility matrix;  $\omega_i$  and  $\mathbf{\Phi}_i$  are the  $i$ th frequency and mass-normalized mode shape, respectively; *s dof* is the number of degrees of freedom. In above equation, the flexibility matrix can be well approximated by using a few low modes as

$$\tilde{\mathbf{F}} = \sum_{i=1}^{n mod} \frac{1}{\omega_i^2} \mathbf{\Phi}_i \mathbf{\Phi}_i^T, \quad (2)$$

where *n mod* is the number of considered low modes. When a structure is damaged, the mode shapes, the frequencies and then the flexibility matrix are changed. Therefore, the change in flexibility matrix has been used as an indicator to detect damage locations. This change can be archived as

$$\tilde{\mathbf{F}}_{\Delta} = \tilde{\mathbf{F}}_{UD} - \tilde{\mathbf{F}}_D, \quad (3)$$

where the indexes *UD* and *D* mean respectively undamaged and damaged structures.

In 2002, Bernal [19] has defined the DLVs as a basis for the null space of the change in flexibility. When DLVs are applied to structures as static loads, there is no stress at damaged elements and some undamaged elements (misidentified elements). Using this characteristic, we can find out the damage locations in structure. The DLVs can be calculated from the singular-value decomposition (SVD) of  $\tilde{\mathbf{F}}_{\Delta}$  as follows

$$\tilde{\mathbf{F}}_{\Delta} \stackrel{SVD}{=} [\mathbf{U}_1 \ \mathbf{U}_0] \begin{bmatrix} \mathbf{\Sigma}_1 & \mathbf{0} \\ \mathbf{0} & \mathbf{0} \end{bmatrix} [\mathbf{V}_1 \ \mathbf{V}_0]^T, \quad \text{with } DLVs = \mathbf{V}_0 \quad (4)$$

where  $\mathbf{\Sigma}_1$  is a diagonal matrix including nonzero singular values of  $\tilde{\mathbf{F}}_{\Delta}$ ;  $[\mathbf{U}_1 \ \mathbf{U}_0]$  and  $[\mathbf{V}_1 \ \mathbf{V}_0]$  are orthogonal matrices.

As mentioned above, DLVs generate zero stress at damaged elements and thus, obviously, it also produces zero strain energy. Consequently, we propose *nei* as a new indicator using strain energy of elements to pinpoint the damage locations. The procedure used to establish the indicator is based on reference [22] in which the modal strain energy is handled as a damage location method. The modal strain energy of an element corresponding to a mode shape can be presented as follows [22]

$$mse_i^e = \frac{1}{2} \mathbf{\Phi}_i^{eT} \mathbf{K}^e \mathbf{\Phi}_i^e, \quad (5)$$

where  $\mathbf{\Phi}^e$  is the  $i$ th mode shape of the  $e$ th element and  $\mathbf{K}^e$  is the  $e$ th element stiffness matrix.

The procedure of formulating *nei* consists of three steps. Firstly, we use displacements of the reference structure under DLVs to compute the so-called damage locating

vector based strain energy ( $dlvse$ ) for each element

$$dlvse_i^e = \frac{1}{2} \mathbf{d}_i^{eT} \mathbf{K}^e \mathbf{d}_i^e, \quad (6)$$

where  $\mathbf{d}_i^e$  is the displacement of the  $e$ th element when the undamaged structure is subjected to the  $i$ th DLV load. Secondly, in order to avoid inaccuracy in damage detection [22], we normalize the  $dlvse_i^e$  with respect to the total strain energy as follows

$$ndlvsse_i^e = \frac{dlvse_i^e}{\sum_{e=1}^{nele} dlvse_i^e}, \quad (7)$$

where  $nele$  is the number of elements. Finally, the normalized energy index ( $nei$ ) is defined for each element by the following equation

$$nei^e = \frac{\sum_{i=1}^{nl} ndlvsse_i^e}{\max_k \left\{ \sum_{i=1}^{nl} ndlvsse_i^k \right\}}, \quad (8)$$

The computed  $nei$  becomes the indicator of structure in DLV method.

From Eqs. (6) (7) and (8) we can see that  $nei$  of damaged elements equal zero for all DLVs due to the feature of DLVs. Unfortunately, besides causing zero stress at damaged elements, each DLV may also cause zero stress at some undamaged elements. If we use only one DLV load,  $nei$  criteria may lead to misidentify some undamaged elements in the set of identified damaged elements. One way to overcome this difficulty is that the  $nei$  should be computed from as many DLVs as possible. Indeed, the DLV loads are applied to the reference model and  $nei$  can be obtained easily by using a convenient finite element analysis (FEA). Hence, we can employ all loads to gain more accurate damage localization.

### 3. NUMERICAL EXAMPLES

To demonstrate the effectiveness of the new proposed indicator, three numerical examples namely: (1) a cantilevered beam, (2) a 2D-planar truss and (3) a 3D truss are considered in this section. Besides, the influence of noise also carried out in these examples. The damaged structures are modeled by reducing the Young's modulus of affected elements. All codes of FEA are written in Matlab (2014a) software.

#### 3.1. Cantilevered beam

In this example, we consider a rectangular aluminum cantilevered which was previously studied to validate a damage location method by Hong Hao et al. [24]. The beam has the length of 495.3 mm, the width of 25.4 mm and the thickness of 6.35 mm. The Young's modulus of the material and the mass density are 71 GPa and 2210 kg/m<sup>3</sup>, respectively. The beam is divided into 20 elements of equal lengths (see Fig. 1). The damage is simulated by reducing in the elemental stiffness matrix at different locations of aluminum cantilevered beam. Two cases of damage are considered as shown in Tab. 1.

In case one only element 9 is reduced 30% of stiffness, while in the second case elements 4 and 8 are respectively reduced 50% and 30% of stiffness. The first six natural frequencies of intact model and damage cases are listed in Tab. 2. In practical measurements vibration data of structures, it is often impossible to avoid the presence of noise in the measurement and it is widely recognized that the natural frequencies are least contaminated by measurement noise and can generally be measured with good accuracy. As it was reported in [22], the frequencies and mode shapes most likely to be contaminated by measurement noise with a standard error of 0.15% and 3% for the modal frequencies and mode shapes, respectively. In this example, the same level of noise for frequency and mode shape is also used for both cases of damage. Besides, the effect of level of noise for mode shapes is investigated with three different levels corresponding with 1%, 2% and 3%.

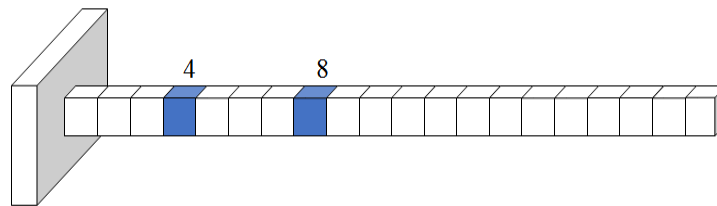


Fig. 1. The sketch of a cantilevered beam which is damaged at elements 4 and 8

Table 1. Two cases of damage in the cantilevered beam

Case 1 (single damage)		Case 2 (multiple damages)	
Element number	Damage ratio	Element number	Damage ratio
9	0.3	4	0.5
		8	0.3

Table 2. The first six natural frequencies for the intact model and two damage cases for the cantilevered beam

Mode	Intact [24]	Intact (Present)	Case 1 (Present)	Case 2 (Present)
1	23.71	23.70	23.51	22.23
2	148.59	148.53	146.06	146.22
3	416.05	415.88	413.53	408.23
4	815.33	815.00	807.25	790.28
5	1347.95	1347.40	1327.86	1277.47
6	2014.01	2013.20	2008.07	1962.38

For investigating influence of number of modes on the magnitude of *nei* values, various numbers of modes (from 1 to 6) are examined as shown in Fig. 2 and Fig. 3 for

case 1 and case 2, respectively. As can be observed from these figures, the actual damaged elements can be distinguished from the others by the magnitude of  $nei$  of all elements except in case of using only the first mode for case 2. It can also be seen that when the number of modes is greater than or equal to 3, the magnitude of  $nei$  at damaged elements is inversely proportional to the number of modes. It means that the larger number of modes is employed, the more accurate the damage identification results are.

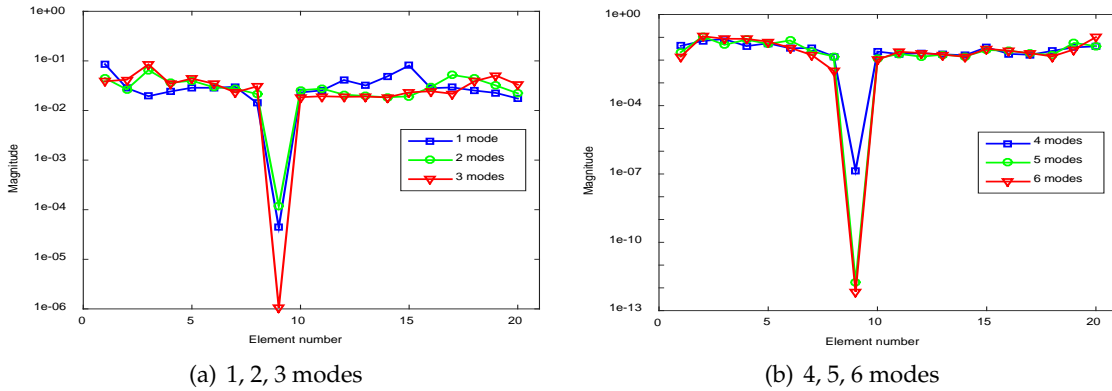


Fig. 2. The  $nei$  values of all elements of the cantilevered beam using the first 1, 2, ..., 5 and 6 modes for case 1

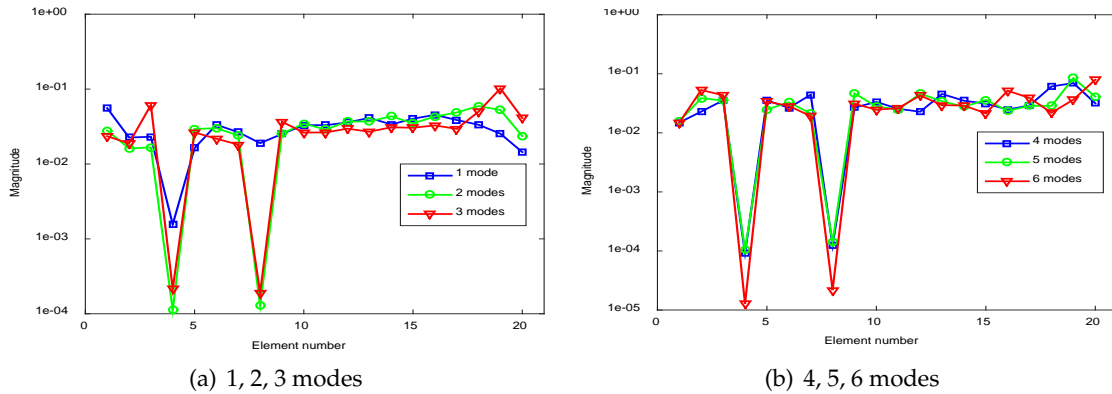


Fig. 3. The  $nei$  values of all elements of the cantilevered beam using the first 1, 2, ..., 5 and 6 modes for case 2

Fig. 4 presents the  $nei$  values of all elements for case 1, when the flexibility matrix is approximated by using different ranges of discrete modes. It can be seen that the magnitude of  $nei$  can identify location of damage when the 1<sup>st</sup>, 2<sup>nd</sup> and 4<sup>th</sup> modes are utilized. However, it is not accurate for the case of the lack of the first one or two modes. This is because the accuracy of the flexibility matrix, approximated by Eq. (1), depends mainly on the first modes.

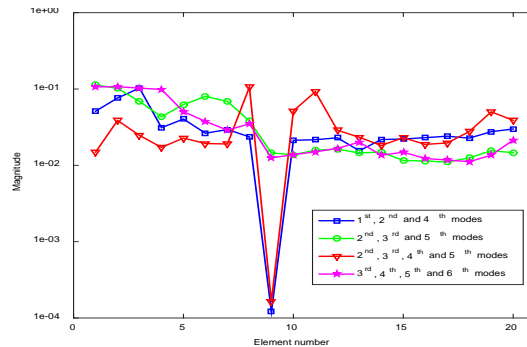


Fig. 4. The *nei* values of all elements with different ranges of discrete modes for case 1

By using the first five modes, the magnitude of *nei* of all elements for two damage cases considering noise as described above is given in Fig. 5. An examination of the figure demonstrates that the *nei* still indicates exact damaged elements for both cases of damage. In addition, the level of error for the mode shapes clearly influences on the magnitude of *nei* of elements. If the standard error is 1%, the *nei* value of damaged elements is the smallest compared with the standard error of 2% and 3%. And, the *nei* values of those elements for standard error of 2% is less than that of those elements for standard error of 3%.

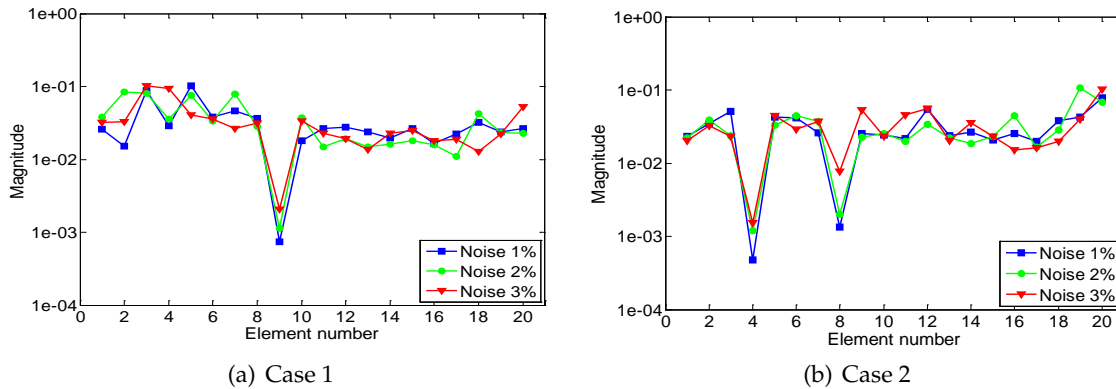


Fig. 5. The *nei* values of all elements of the cantilevered beam for two damage cases considering noise, 0.15% for frequencies and 1%, 2% and 3% for mode shapes

### 3.2. 2D-planar truss

In this example, a 14-bay planar truss is considered to investigate the effectiveness of the proposed indicator. This truss model has been employed to verify a new mode accuracy indicator for eigensystem realization analysis (ERA) method by Gun Jin Gun et al. [24]. The planar truss consists of 53 steel bars and 28 nodes as shown in Fig. 6. All bars have the same material properties that are Young’s modulus 199 GPa and the mass

density  $7827 \text{ kg/m}^3$ . The member of each bar is a tubular cross-section having an inner diameter of 3.1 mm and an outer diameter of 17.0 mm. Total length of the truss is 5.6 m with 0.4 m in each bay, and the high of structure is 0.4 m. Two damage cases, listed in Tab. 3, are numerically simulated here by reducing the elemental stiffness matrix at different positions. The first ten natural frequencies of the intact model and two damage cases for the truss are listed in Tab. 4. The noise is added into frequencies and mode shapes for both cases of damage as in the previous example.

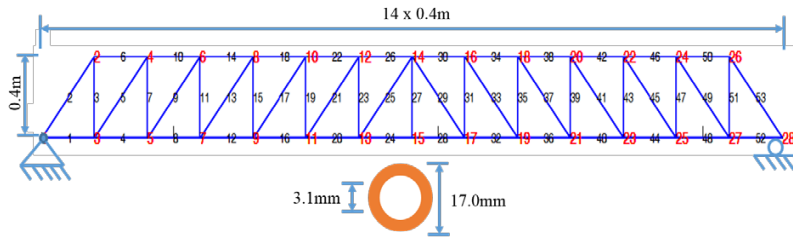


Fig. 6. Sketch of a 14-bay planar truss

Table 3. Two cases of damage in the 14-bay planar truss

Case 1 (single damage)		Case 2 (multiple damages)	
Element number	Damage ratio	Element number	Damage ratio
18	0.4	8	0.2
		18	0.4
		31	0.5

Table 4. The first ten natural frequencies for the intact model and two damage cases for the 14-bay planar truss

Mode	Intact (Lab) [25]	Intact (ERA) [25]	Intact (Present)	Case 1 (Present)	Case 2 (Present)
1	31.94	31.97	31.93	31.53	31.42
2	108.72	108.65	108.76	108.00	106.57
3	-	-	157.39	153.06	152.03
4	-	-	217.29	216.12	214.86
5	333.41	333.35	333.36	333.20	331.88
6	444.16	444.20	444.08	442.36	438.19
7	-	-	454.64	454.63	454.30
8	-	-	558.68	557.18	555.50
9	-	-	648.07	647.74	640.24
10	725.12	725.02	725.00	708.96	703.99



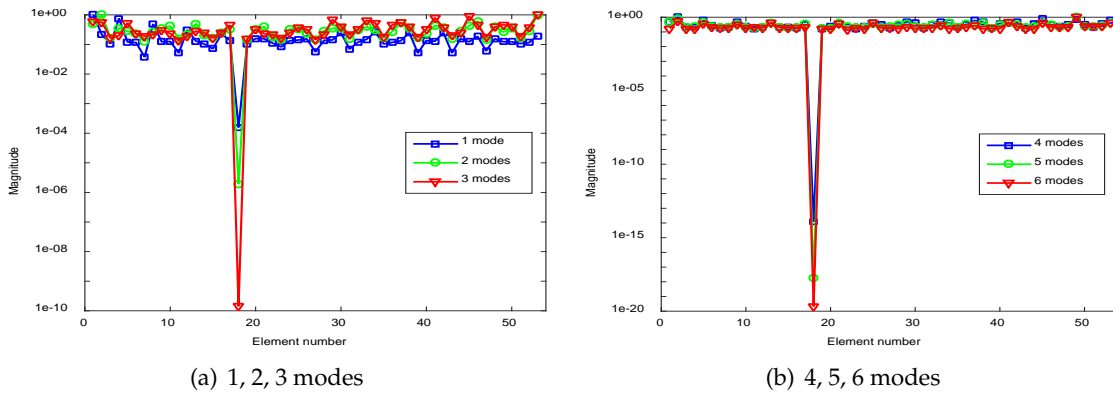


Fig. 7. The *nei* values of all elements of the 14-bay planar truss using the first 1, 2, ..., 5 and 6 modes for case 1

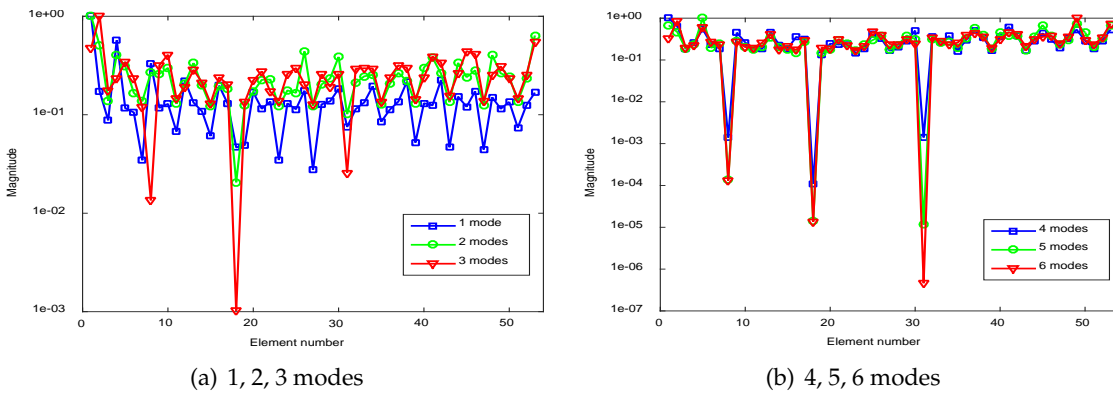


Fig. 8. The *nei* values of all elements of the 14-bay planar truss using the first 1, 2, ..., 5 and 6 modes for case 2

For both two damage cases of the truss, the influence of the number of modes for approximating the flexibility matrix on the magnitude of the *nei* values of all elements is investigated as shown in Fig. 7 and Fig. 8. Particularly, the first 1, 2, ..., 5 and 6 modes are considered. In Fig. 7, the values of *nei* at the element 18 are almost the same and identically to zero in the case of more than one mode, while in case of one mode, it is larger than the other cases but still too small. Fig. 8 shows that when number of modes is larger than 2, the line graphs at elements 8, 18 and 31 appear three prominent peaks which represent the distinction between damaged elements and the others. On the other hand, when only the first mode or the first two modes is used the *nei* values may not be accurate for identifying multiple damages. Similar to the previous example, it can also be realized that the increasing of number of modes leads to the decreasing of the values of *nei* at damaged elements, when number of modes is larger than or equal to 3.

A comparison between the *nei* and *ncs* for case 1 is shown in Fig. 9. Here, the *ncs* which is calculated based on cumulative stress of elements is firstly proposed by Bernal

et al. [19] as an indicator for detecting damage in the DLV method. Both indexes are computed using the first 5 modes. It can be seen in Fig. 9 that the *nei* and *ncs* magnitudes at the 18th element are very small. However, the value of *nei* at the element is smaller than *ncs*. It is reasonable result since the *nei* is computed based on strain energy [21].

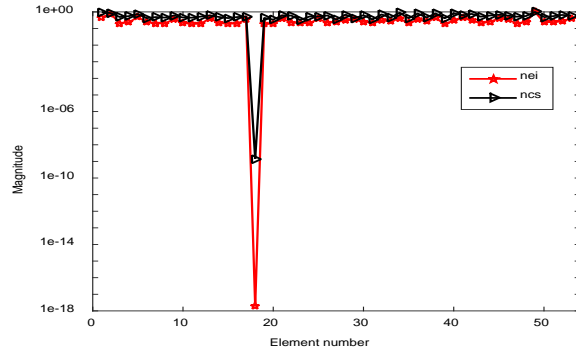


Fig. 9. Comparison between the *nei* and *ncs* values of all elements of 14-bay planar truss for case 1

In the case of additive noise, the *nei* values of all elements for both cases using 5 modes are depicted in Fig. 10. According to the value of *nei*, the damaged elements is still identified for two lower level of error (0.15% for frequencies, 1% and 2% for mode shapes). When the mode shapes are added by 3% of noise, in case 2 (two damaged elements), the value of *nei* may lead to some mistakes for locating damaged elements.

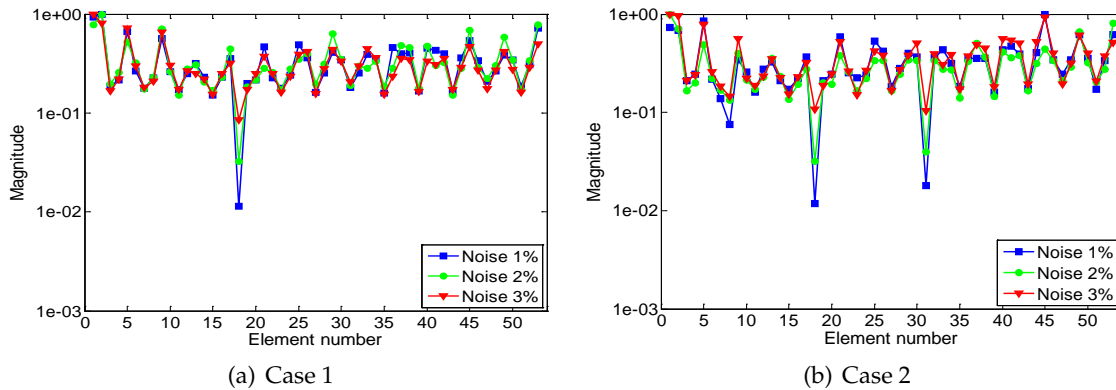


Fig. 10. The *nei* values of all elements of the 14-bay planar truss for two damage cases considering noise, 0.15% for frequencies and 1%, 2% and 3% for mode shapes

### 3.3. 72-bar space truss

The third example is a 72-bar space truss (see Fig. 11), as referred to [26]. This truss has four non-structural masses attached at nodes 1-4. Material properties of the truss and the value of added masses are provided in Tab. 5. The cross section of each element group

shown in Tab. 6 is taken from the optimal result of [26]. The detail of a damage case with multiple damage scenarios is given in Tab. 7. The first five frequencies of undamaged and damaged structure are presented in Tab. 8.

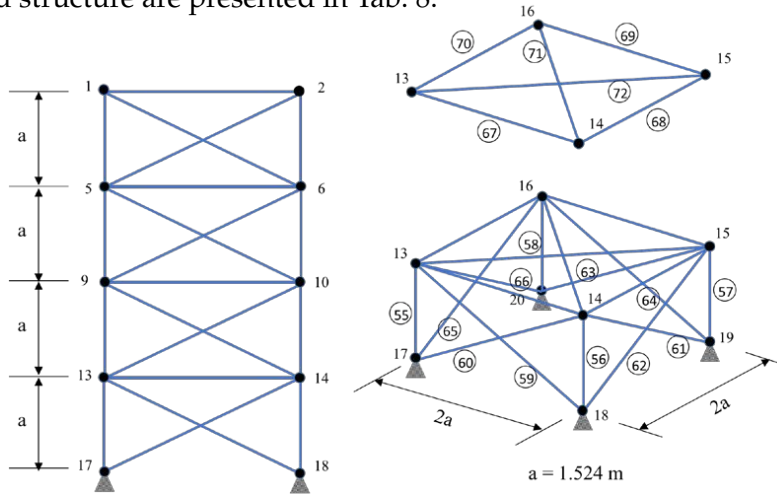


Fig. 11. A sketch of a 72-bar space truss

Table 5. Material properties of the 72-bar space truss

Property/unit	Value
$E$ (Young's modulus)/N/m <sup>2</sup>	6.98e10
$\rho$ (Mass density)/Kg/m <sup>3</sup>	2770
Added mass/Kg	2270

Table 6. Cross-sectional areas (cm<sup>2</sup>) for 16 element groups of the 72-bar space truss

Element group	Cross-sectional area	Element group	Cross-sectional area
1-4	2.854	37-40	16.328
5-12	8.301	41-48	8.299
13-16	0.645	49-52	0.645
17-18	0.645	53-54	0.645
19-22	8.202	55-58	15.048
23-30	7.043	59-66	8.268
31-34	0.645	67-70	0.645
35-36	0.645	71-72	0.645

The  $nei$  values of all elements of the truss for various numbers of modes are depicted in Fig. 12. As can be seen in Fig. 12, the values of  $nei$  at elements 7 and 9 are much smaller than those of the others for the cases of more than one mode. Therefore, these elements can be determined as the damaged elements. Again, as in the previous examples, the accuracy of  $nei$  in detection of damage location is influenced by number of modes.

Table 7. A damage case for the 72-bar space truss

Element number	Damage ratio
7	0.1
9	0.3

Table 8. The first five frequencies (Hz) of the 72-bar space truss for undamaged and damaged structures

Mode	Intact [26]	Intact (present)	Damaged (present)
1	4.000	4.0003	3.9798
2	4.000	4.0003	3.9949
3	6.004	6.0002	5.9532
4	6.2491	6.2496	6.2425
5	8.9726	8.9728	8.9080
6	-	9.0041	8.9705

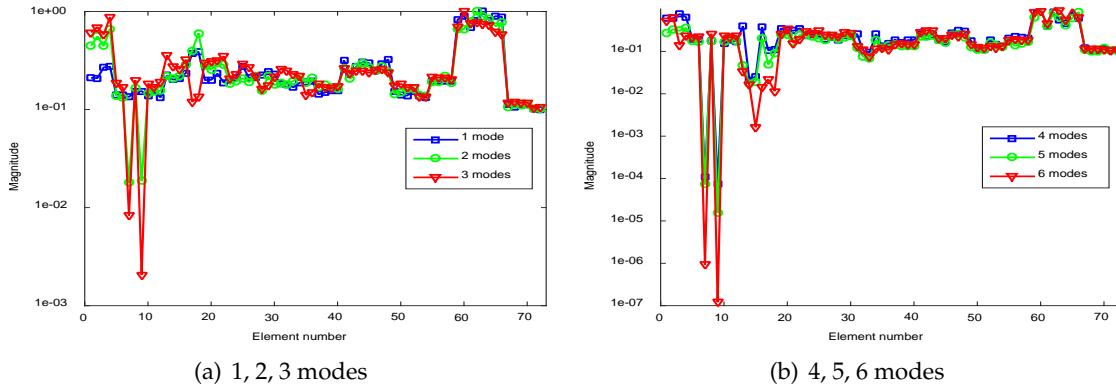


Fig. 12. The *nei* values of all elements of the 72-bar space truss using the first 1, 2, . . . , 5 and 6 modes

#### 4. CONCLUSION

In this study, a so-called normalized energy index (*nei*) is defined and applied to structural damage detection. The indicator is calculated based on the cumulative strain energy at elements of structure. The efficiency of the proposed indicator in multiple damage detection is demonstrated through three numerical examples of beam and truss structures. The results show that for both types of structures, *nei* can identify successfully multiple damage cases even when only first few modes are used. Moreover, the indicator also gives good result when measurement data is added by random noise. The numerical results also indicate that the accuracy of the *nei* for damage identification is influenced

by number of modes i.e. the larger number of modes is, the more accurate the damage identification results are.

Although the indicator *nei* has demonstrated its effectiveness in damage identification for beam and truss structures, it still remains some limits.

In case of using only the first mode, the *nei* may not identify multiple damage locations correctly.

Under the effect of high level of noise, the *nei* requires larger number of modes to precisely locate the damage.

Besides, *nei* can predict damage by using a first few modes; however, this advantage may not be effective in case of the lack of some these first modes.

The results obtained in this paper will be extend for further researches such as investigating the influence of damage feature on accuracy and reliability of the proposed methods.

#### ACKNOWLEDGEMENTS

This research is funded by Vietnam National University Ho Chi Minh City (VNU-HCM) under grant number B2013-18-03.

#### REFERENCES

- [1] P. Cawley and R. D. Adams. The location of defects in structures from measurements of natural frequencies. *The Journal of Strain Analysis for Engineering Design*, **14**, (2), (1979), pp. 49–57.
- [2] O. S. Salawu and C. Williams. Bridge assessment using forced-vibration testing. *Journal of Structural Engineering*, **121**, (2), (1995), pp. 161–173.
- [3] R. J. Allemang and D. L. Brown. A correlation coefficient for modal vector analysis. In *Proceedings of the 1st International Modal Analysis Conference*, Vol. 1. SEM, Orlando, (1982), pp. 110–116.
- [4] A. K. Pandey, M. Biswas, and M. M. Samman. Damage detection from changes in curvature mode shapes. *Journal of Sound and Vibration*, **145**, (2), (1991), pp. 321–332.
- [5] Q. Lu, G. Ren, and Y. Zhao. Multiple damage location with flexibility curvature and relative frequency change for beam structures. *Journal of Sound and Vibration*, **253**, (5), (2002), pp. 1101–1114.
- [6] A. Pandey and M. Biswas. Damage detection in structures using changes in flexibility. *Journal of Sound and Vibration*, **169**, (1), (1994), pp. 3–17.
- [7] B. Jaishi and W.-X. Ren. Damage detection by finite element model updating using modal flexibility residual. *Journal of Sound and Vibration*, **290**, (1), (2006), pp. 369–387.
- [8] N. Stubbs, J. Kim, and K. Topole. An efficient and robust algorithm for damage localization in offshore platforms. In *Proceedings of the ASCE tenth Structures Congress*, (1992), pp. 543–546.
- [9] S. W. Doebling, C. R. Farrar, M. B. Prime, and D. W. Shevitz. Damage identification and health monitoring of structural and mechanical systems from changes in their vibration characteristics: a literature review. Technical report, Los Alamos National Laboratory (United States), (1996).
- [10] E. P. Carden and P. Fanning. Vibration based condition monitoring: A review. *Structural Health Monitoring*, **3**, (4), (2004), pp. 355–377.

- [11] Y. J. Yan, L. Cheng, Z. Y. Wu, and L. H. Yam. Development in vibration-based structural damage detection technique. *Mechanical Systems and Signal Processing*, **21**, (5), (2007), pp. 2198–2211.
- [12] S. W. Smith and C. A. Beattie. Model correlation and damage location for large space truss structures: secant method development and evaluation. Technical report, Virginia Polytechnic Inst. and State Univ., Dept. of Engineering Science and Mechanics., Blacksburg, VA, United States, (1991).
- [13] D. C. Zimmerman and S. W. Smith. Model refinement and damage location for intelligent structures. In *Intelligent Structural Systems*. Springer, (1992), pp. 403–452.
- [14] Z. Sun and C. C. Chang. Structural damage assessment based on wavelet packet transform. *Journal of Structural Engineering*, **128**, (10), (2002), pp. 1354–1361.
- [15] N. Q. Han and N. T. H. Luong. Damage assessment of frame structures using wavelet transform and genetic algorithm. In *The 10th National Conference on Solid Mechanics, Vietnam*, (2010). (in Vietnamese).
- [16] K. V. Nguyen and H. T. Tran. Multi-cracks detection of a beam-like structure based on the on-vehicle vibration signal and wavelet analysis. *Journal of Sound and Vibration*, **329**, (21), (2010), pp. 4455–4465.
- [17] J. N. Kudva, N. Munir, and P. W. Tan. Damage detection in smart structures using neural networks and finite-element analyses. *Smart Materials and Structures*, **1**, (2), (1992), pp. 108–112.
- [18] X. Wu, J. Ghaboussi, and J. H. Garrett. Use of neural networks in detection of structural damage. *Computers & Structures*, **42**, (4), (1992), pp. 649–659.
- [19] D. Bernal. Load vectors for damage localization. *Journal of Engineering Mechanics*, **128**, (1), (2002), pp. 7–14.
- [20] Y. Gao, B. F. Spencer Jr, and D. Bernal. Experimental verification of the flexibility-based damage locating vector method. *Journal of Engineering Mechanics*, **133**, (10), (2007), pp. 1043–1049.
- [21] S. T. Quek, V. A. Tran, X. Y. Hou, and W. H. Duan. Structural damage detection using enhanced damage locating vector method with limited wireless sensors. *Journal of Sound and Vibration*, **328**, (4), (2009), pp. 411–427.
- [22] S. M. Seyedpoor. A two stage method for structural damage detection using a modal strain energy based index and particle swarm optimization. *International Journal of Non-Linear Mechanics*, **47**, (1), (2012), pp. 1–8.
- [23] M. Nobahari and S. M. Seyedpoor. An efficient method for structural damage localization based on the concepts of flexibility matrix and strain energy of a structure. *Structural Engineering and Mechanics*, **46**, (2), (2013), pp. 231–244.
- [24] H. Hao and Y. Xia. Vibration-based damage detection of structures by genetic algorithm. *Journal of Computing in Civil Engineering*, **16**, (3), (2002), pp. 222–229.
- [25] G. J. Yun, S.-G. Lee, and S. Shang. An improved mode accuracy indicator for Eigensystem Realization Analysis (ERA) techniques. *KSCE Journal of Civil Engineering*, **16**, (3), (2012), pp. 377–387.
- [26] A. Kaveh and A. Zolghadr. Truss optimization with natural frequency constraints using a hybridized CSS-BBBC algorithm with trap recognition capability. *Computers & Structures*, **102**, (2012), pp. 14–27.